Geophysical Research Letters

RESEARCH LETTER
10.1029/2024GL113366

Western Pacific Warm Pool $\delta^{18}O$ Response to the El Niño-Southern Oscillation

N. K. Murray[1], J. L. Conroy[1], P. L. Colin[2], K. M. Cobb[3], and D. C. Noone[4]

[1]Department of Earth Science & Environmental Change, University of Illinois Urbana-Champaign, Urbana, IL, USA, [2]Coral Reef Research Foundation, Koror, Palau, [3]Brown University, Institute at Brown for Environment and Society, Providence, RI, USA, [4]Department of Physics, University of Auckland, Auckland, New Zealand

Key Points:

- Palau seawater isotope values track Palau precipitation isotope values and pan-tropical Pacific hydroclimate related to El Niño Southern Oscillation (ENSO)
- Palau seawater isotope - salinity slopes change with ENSO phase

Supporting Information:

Supporting Information may be found in the online version of this article.

Correspondence to:

N. K. Murray and J. L. Conroy,
nkmurray@hawaii.edu;
jconro@illinois.edu

Citation:

Murray, N. K., Conroy, J. L., Colin, P. L., Cobb, K. M., & Noone, D. C. (2025). Western pacific warm pool $\delta^{18}O$ response to the El Niño-Southern Oscillation. *Geophysical Research Letters*, *52*, e2024GL113366. https://doi.org/10.1029/2024GL113366

Received 1 NOV 2024
Accepted 7 JAN 2025

Abstract Tropical Pacific seawater and precipitation stable oxygen isotope data aid in understanding modern oceanic and atmospheric interactions, and these data are particularly valuable as they are archived in isotope-based paleoclimate records. However, the absence of modern seawater isotope time series limits the ability to identify the atmospheric influences on these data, precluding robust paleoclimate interpretations. We present a new 10 year sub-monthly record of seawater and precipitation stable oxygen isotope values ($\delta^{18}O_{sw}$ and $\delta^{18}O_p$) from Koror, Palau. Our dataset indicates that temporally, $\delta^{18}O_{sw}$ is strongly influenced by local $\delta^{18}O_p$. Both monthly $\delta^{18}O_{sw}$ and $\delta^{18}O_p$ are highly correlated with outgoing longwave radiation across the tropical Pacific, reflecting a Walker Circulation imprint on the surface ocean. Changes in the Palau $\delta^{18}O_{sw}$—salinity relationship correspond to NINO3.4 variability, indicating a difference in how these variables record El Niño Southern Oscillation (ENSO) information, but demonstrating the utility of $\delta^{18}O_{sw}$ to reconstruct ENSO variability in the western tropical Pacific.

Plain Language Summary The Western Pacific Warm Pool is a region of the tropical Pacific ocean that experiences large changes in ocean and atmospheric conditions in response to the ENSO. This region is also home to many marine paleoclimate proxies that record climate changes on ENSO timescales, making it an ideal location to look at ENSO variability and influence through time. Stable isotopes act as the 'common currency' that allow us to make connections between modern hydroclimate and paleoclimate records. This study utilizes one of the longest, paired stable isotope records from precipitation and seawater to understand how ENSO variability is reflected in modern western Pacific isotope data and subsequently in isotope-based proxies. The longitudinal data here present a strong, constructive ENSO signal from the ocean and atmosphere, showing that western Pacific paleoclimate proxies should reliably record ENSO variability through time.

1. Introduction

Seawater oxygen isotope data ($\delta^{18}O_{sw}$) can provide numerous insights into atmospheric and oceanic processes (Akhoudas et al., 2021; Bauch et al., 1995, 2005; Conroy et al., 2023; Dubinina et al., 2017; Reyes-Macaya et al., 2022). Freshwater fluxes (evaporation and precipitation) to the ocean surface are known to influence mixed layer $\delta^{18}O_{sw}$, which is reflected in its linear relationship with mixed layer salinity (Conroy et al., 2017, 2023; Murray et al., 2023; Reed et al., 2022; Thompson et al., 2022). However, $\delta^{18}O_{sw}$ is susceptible to further influences from the atmosphere that salinity is not, as salinity cannot integrate the varying isotopic values of precipitation inputs, which can reflect multiple moisture-related processes (Konecky et al., 2019).

The extent to which precipitation $\delta^{18}O$ ($\delta^{18}O_p$) influences $\delta^{18}O_{sw}$ is largely unknown due, in part, to the dearth of available observational data. One long-term monitoring study from the eastern tropical Pacific revealed that $\delta^{18}O_{sw}$ does not record a significant atmospheric influence, and instead records Pacific Equatorial Undercurrent variability on monthly timescales (Conroy et al., 2023). However, unlike the eastern tropical Pacific, the western tropical Pacific is a region with large-scale atmospheric convergence, high precipitation rates, and overall lower $\delta^{18}O_p$ values (Conroy et al., 2017; Falster et al., 2021; Konecky et al., 2019). These differences in hydroclimate should translate to a sizable impact on surface ocean $\delta^{18}O_{sw}$.

If western tropical Pacific hydroclimate variability does influence $\delta^{18}O_{sw}$, there is potential to derive long-term hydroclimate information from $\delta^{18}O_{sw}$ values, and proxies for $\delta^{18}O_{sw}$ values. Such hydroclimate information may also be broad-scale, rather than local, as $\delta^{18}O_p$ values are increasingly shown to be a measure of regional scale changes in atmospheric circulation and moisture source changes, rather than simply relating to local

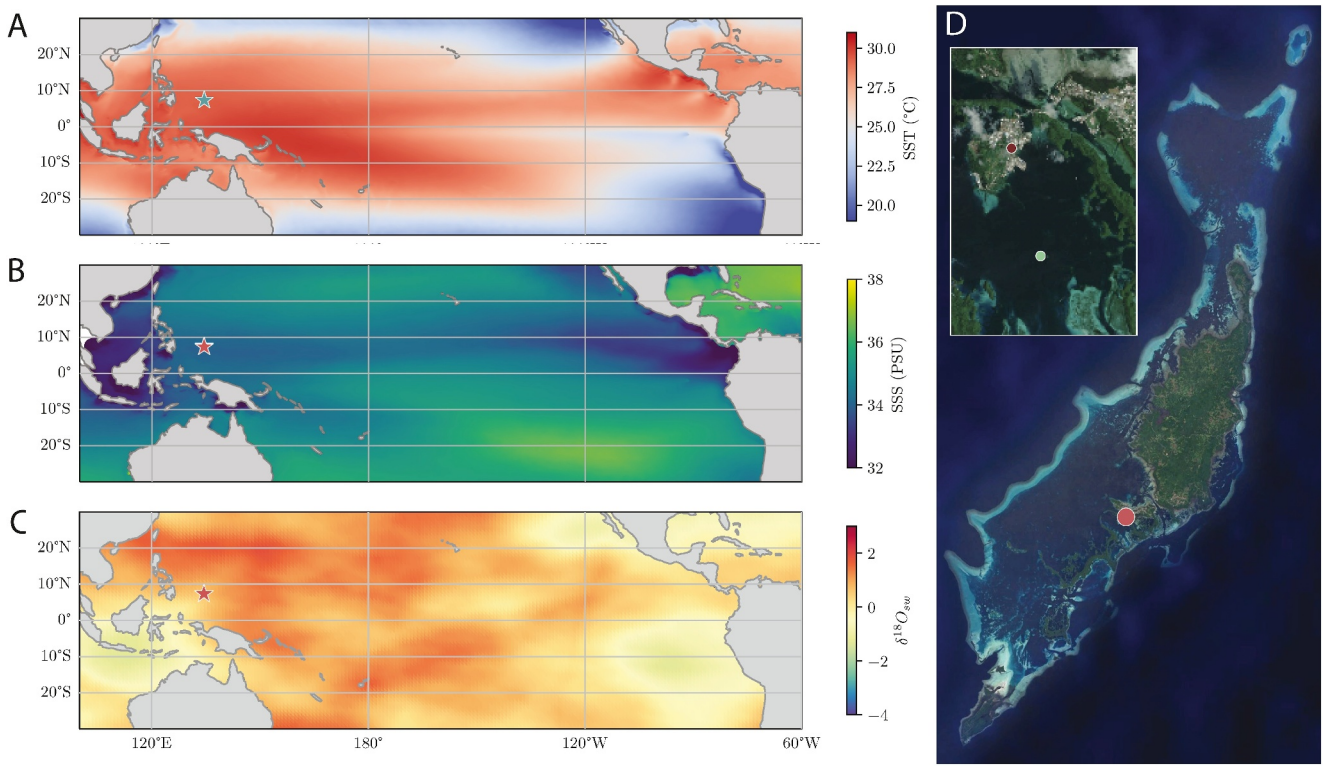

Figure 1. Map showing Palau (red star), and regional, monthly averaged (a) sea surface temperature (HadISST, Rayner et al., 2003) (b) SSS (GLORYS12, Jean-Michel et al., 2021) and (c) Interpolated mixed layer $\delta^{18}O_{sw}$ (Murray et al., 2023) for the tropical Pacific Ocean. (d) Palau aerial map with (Coral Reef Research Foundation) site shown in red (Google Earth, 2024). Inset image shows Malakal Harbor, Palau with green dot indicating the seawater collection location.

processes such as precipitation amount (Kukla et al., 2024). In the tropical Pacific, regional scale changes in hydroclimate and $\delta^{18}O_p$ are closely related to the El Niño-Southern Oscillation (ENSO) on interannual timescales (e.g., Conroy et al., 2013; Martin et al., 2018; Moerman et al., 2013; Permana et al., 2016). However, the extent to which this information is inherited by the surface ocean, and subsequent marine paleoclimate proxies, remains an open question requiring a long-term precipitation and seawater isotope data. Modern $\delta^{18}O$ observational campaigns, though temporally limited, indeed record ENSO responses in western Pacific precipitation and seawater (Horikawa et al., 2023; Permana et al., 2016). Thus, if there is a robust relationship between $\delta^{18}O_p$ and $\delta^{18}O_{sw}$, this framework can be applied to marine paleoclimate records to reconstruct interannual hydroclimate variability associated with ENSO through time.

Here, we present a 10 year sub-monthly record of paired precipitation and seawater $\delta^{18}O$ values from Koror, Palau in the Western Pacific Warm Pool (WPWP) of the tropical Pacific. Palau experiences complex changes in atmospheric convergence and ocean circulation related to ENSO variability on interannual timescales. Several paleoclimate records have been developed from Palau marine carbonate archives, including corals, clams, and sclerosponges (Grottoli et al., 2010; Osborne et al., 2014; Wen et al., 2024; Wu & Grottoli, 2010). Our investigation of one of the longest, paired time series of $\delta^{18}O_p$ and $\delta^{18}O_{sw}$ values reveals the influence of ENSO and has implications for the interpretation of the numerous isotope-influenced marine paleoclimate records in the region.

2. Study Site and Methodology

The Republic of Palau is in the western tropical Pacific at ~7.3°N, 134.5°E (Figure 1) within the WPWP. The WPWP drives significant heat redistribution across the globe, leading to changes in climate and ocean circulation. Situated in northwestern WPWP, Palau is subject to persistently high sea surface temperature (SST) that rarely drops below 28°C, high annual precipitation rates, and a deep thermocline (Figure S1 in Supporting Information S1). Interannual climate variability in the WPWP is associated with ENSO, and this region experiences

especially large precipitation changes related to ENSO variability (Osborne et al., 2013). Reduced precipitation during El Niño events is severe enough to induce drought and wildfire in Palau (Dendy et al., 2022).

The long-term collection site for this study is situated in Koror, the northern and most populous state in the Palauan Archipelago (Figure 1). Samples were collected from February 2013 - December 2023 at the Coral Reef Research Foundation (CRRF, 7.32°N 134.46°E) (Figure 1). The record is nearly continuous, with a brief gap in the dataset in 2015 where samples were lost due to a fire at CRRF. Precipitation samples were collected daily at CRRF adjacent to Malakal Harbor using a 1L separatory funnel with mineral oil as a barrier to evaporation (Conroy et al., 2016; Martin et al., 2018). Weekly or bi-weekly, the CRRF staff collected seawater samples by boat in nearby Malakal Harbor (7° 19.008' N; 134° 27.627') (Figure 1).

2.1. Sample Measurement

2.1.1. Seawater

Seawater samples span February 2013 - March 2023 and were measured for $\delta^{18}O$, $\delta^{2}H$ and salinity. Samples used for salinity measurements were collected in 60 ml amber Nalgene™ bottles and parafilmed. Samples for isotope analyses were collected in 3.5 ml glass vials with butyl stoppers and sealed with aluminum crimp tops. Prior to September 2020, salinity measurements were obtained using a Thermo Scientific Orion Star A212 benchtop conductivity meter and were an average of five measurements at 25°C. The meter was calibrated every 10 samples using a 50.0 mS/cm certified conductivity solution. From October 2020 onward, the Guildline Autosal 8400 B (<±0.002 PSU) was used to measure seawater salinity. Standardization and calibration were done using IAPSO standard seawater (34.994 PSU) before each batch of measurements. There was no statistically significant offset in the salinity data after the change in instrument in October 2020, though measurement period of the Autosal instrument may be too short to robust detect change (Supplemental Figure S3 in Supporting Information S1). A subset of this data (2013–2016 seawater) was previously published by Conroy et al. (2017) and the data presented here represents continued sample collection at Palau. Seawater salinity and isotope data were both averaged into monthly values for the analyses presented here.

Isotope measurements from February 2013 until April 2016 were done using a Picarro L-2130i, whereafter an L-2140i was used. Each datapoint represents the average of six injections, and seawater samples were filtered using 0.45 μm filters to reduce syringe clogging prior to measurement. Raw isotope measurements were calibrated to Greenland Ice Sheet Project, Standard Light Antarctic Precipitation 2 and Vienna Standard Mean Ocean Water 2 standards using three 'in-house' standards. Data was corrected for drift and memory effects after van Geldern and Barth (2012). Instrumental error is 0.1‰ for $\delta^{18}O$ and 0.8‰ for $\delta^{2}H$.

2.1.2. Precipitation

Daily precipitation samples for $\delta^{18}O/\delta^{2}H$ analyses were stored in 3.5 ml glass crimp top vials with butyl stoppers and span February 2013—December 2023. Isotope measurements followed the protocol for seawater delineated above, using only five injections. Precipitation samples are not filtered prior to measurement. Raw isotope measurements were calibrated and corrected for drift and memory following the same protocol as seawater samples. Precipitation data were converted from daily to amount-weighted monthly values using the daily CRRF station precipitation totals.

Several climate data sources that are assessed alongside precipitation and seawater isotope data and statistical analyses are delineated in detail in the supplemental text in Supporting Information S1.

3. Results

3.1. Seawater Isotope and Salinity Results

We present 288 seawater samples with measurements for salinity and $\delta^{18}O_{sw}$ from February 2013 to March 2023, and all mean values reported are over this date range. Seawater $\delta^{18}O$ ranges from −0.37 to 0.39‰ (mean 0.03 ± 0.15‰) and salinity values range from 32.33 to 34.61 PSU (mean 33.66 ± 0.43 PSU). 1 sigma values are reported throughout. Monthly average $\delta^{18}O_{sw}$ values range from −0.29 to 0.37 ‰ ($N = 97$, mean 0.04 ± 0.13‰) and monthly average salinity ranges from 32.33 to 34.58 PSU ($N = 97$, mean 33.69 ± 0.40 PSU). Monthly average seawater $\delta^{18}O_{sw}$ values are significantly correlated with salinity ($r = 0.71$) and Palau precipitation $\delta^{18}O$

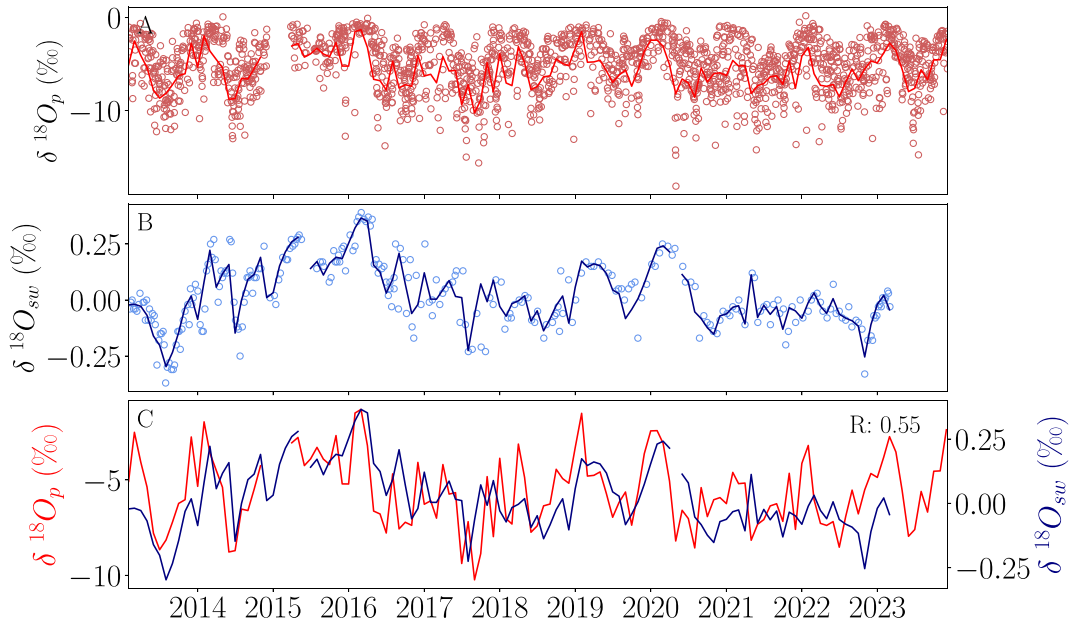

Figure 2. Time series of (a) $\delta^{18}O_p$ and (b) $\delta^{18}O_{sw}$ data from Koror, Palau. Circles represent individual datapoints and lines show monthly means for each variable. Time series of monthly mean values as in (a) and (b) shown together in (c) with Pearson's correlation coefficient in upper right corner.

(r = 0.55) over the sampling period (Figure 2). Monthly $\delta^{18}O_{sw}$ data are also highly correlated with NINO3.4 (r = 0.55, Figure S4 in Supporting Information S1). Spatially, $\delta^{18}O_{sw}$ is correlated with outgoing longwave radiation (OLR) across the tropics, though negatively in the central-east (r = ∼−0.6-0.8) and positively in the west (r = ∼0.5–0.7). Over the collection site, the $\delta^{18}O_{sw}$—OLR correlation is strong and positive (r = 0.51, Figure 3).

The $\delta^{18}O_{sw}$—salinity relationship for the 2013–2023 monthly data from Palau has a slope of 0.26 (±0.05 ‰/PSU) and an intercept ('freshwater endmember') of −8.74 (±1.61‰) (note that these values are different than

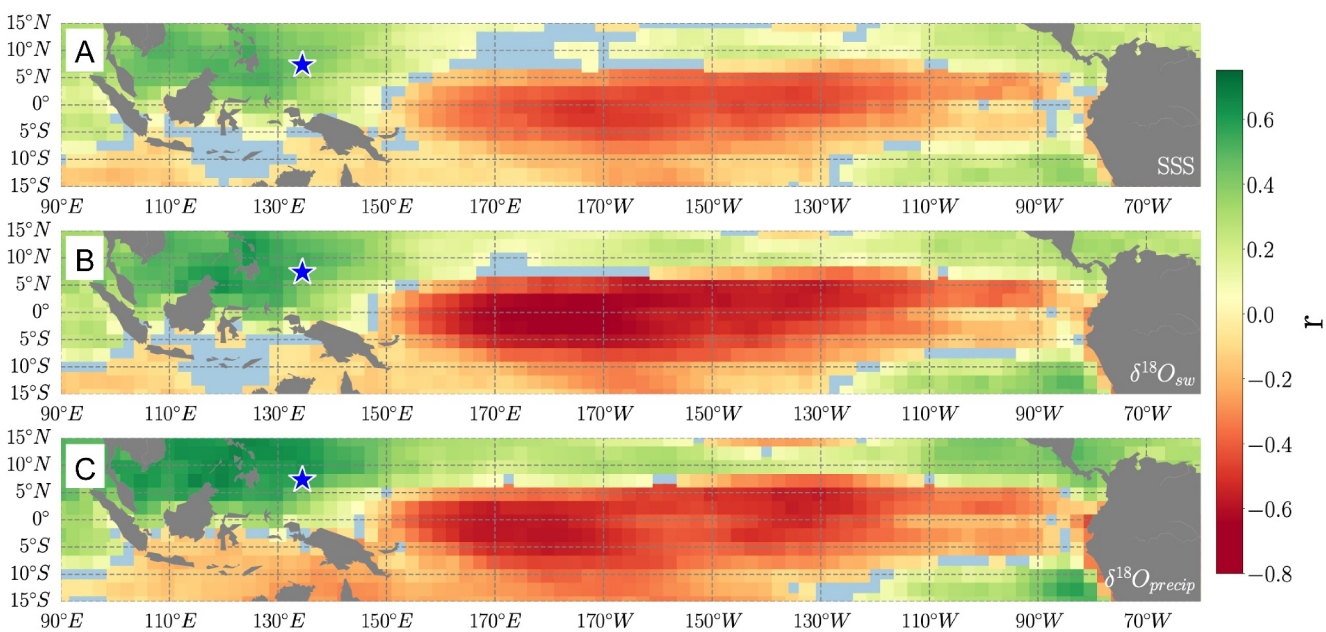

Figure 3. Map of correlation coefficients for monthly averaged outgoing longwave radiation (OLR, Liebmann & Smith, 1996) and Palau (a) salinity, (b) $\delta^{18}O_{sw}$, and (c) $\delta^{18}O_{precipitation}$ across the tropical Pacific from February 2013 to December 2023. Non-significant grid points are removed (blue).

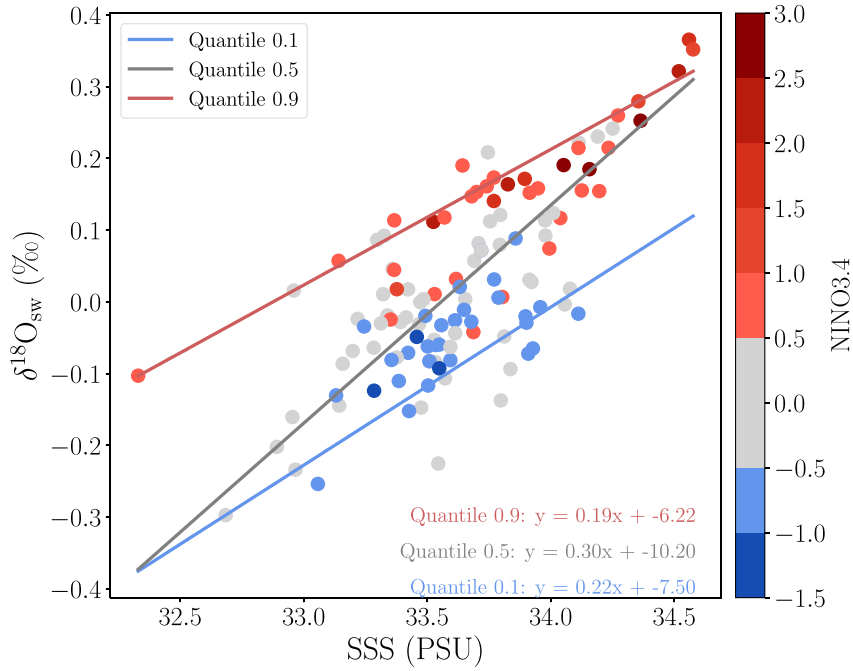

Figure 4. Scatterplots of monthly averaged Palau $\delta^{18}O_{sw}$ and SSS. Colors show monthly NIÑO 3.4 values. 10th, 50th and 90th percentile linear regressions of $\delta^{18}O_{sw}$—salinity reported on bottom right. Alternative visualizations of $\delta^{18}O_{sw}$, SSS are shown in Figure S13 in Supporting Information S1.

the slopes reported in Figure 4, which shows quantile regressions). This is a higher slope and lower intercept compared to the eastern Pacific, consistent with previous findings across the tropical Pacific (Conroy et al., 2014, 2017, 2023). Previous work has provided $\delta^{18}O_{sw}$—salinity data for 1998–2000 and 2013–2016 in Palau (Conroy et al., 2017; Morimoto et al., 2002); both of which report higher slopes and lower intercepts than the dataset presented here. Considering the slope of each of these datasets the Palau $\delta^{18}O_{sw}$—salinity slope has been decreasing since 1998–2000 (Figure S5 in Supporting Information S1). Overall, there is considerable variability in the $\delta^{18}O_{sw}$—salinity relationship year to year in the slope, intercept and R^2, with some years having an R^2 value close to zero (Figure S6 in Supporting Information S1).

Monthly $\delta^{18}O_{sw}$ is also highly correlated with western Pacific regional circulation (Figures S7, S8 in Supporting Information S1). Correlations with upper 150 m ocean velocities peak in the region west of Palau, on the Philippine coast, and the region just south of Palau (Figure S7 in Supporting Information S1). These correlations occur in the mean locations of the Mindanao Current (MC) and the Northern Equatorial Counter Current (NECC). The direction of the correlation is negative at the MC and positive at the NECC. The conventions of current direction dictate that a strong MC is a highly negative V (southward flow) and a strong NECC is a highly positive U value (eastward flow), therefore both correlations amount to the same effect: higher $\delta^{18}O_{sw}$ when the MC and the NECC are stronger.

3.2. Precipitation Results

$\delta^{18}O$ and $\delta^{2}H$ are reported for 1923 precipitation samples spanning February 2013 to December 2023. $\delta^{18}O_p$ ranges from −18.11 to 0.07‰ (mean −4.99 ± 2.91‰) and $\delta^{2}H_p$ values range from −134.78 to 10.70‰ (mean −27.99 ± 23.22‰). Amount weighted monthly average $\delta^{18}O_p$ values ranges from −10.23 to −1.31 ‰ ($N = 87$, mean −5.50 ± 2.03‰) and $\delta^{2}H_p$ ranges from −67.58 to 1.53 ‰ ($N = 87$, mean −31.62 ± 15.93 ‰). The local meteoric water line here is $\delta^{2}H = 7.80\ (\delta^{18}O) + 11.40$, a slightly lower slope and higher intercept than the global meteoric water line. $\delta^{18}O_p$, $\delta^{18}O_{sw}$ and salinity all show strong seasonality with a May-October warm, wet season and a November-April cool, dry season (Figure S1 in Supporting Information S1). $\delta^{18}O_p$ decreases during May-October, as does $\delta^{18}O_{sw}$. Outgoing longwave radiation also reaches its minimum during this time, when convective activity and precipitation peaks (Figure S1 in Supporting Information S1).

Palau $\delta^{18}O_p$ is correlated with the NINO3.4 index from 2002 to 2020 (Figure S9 in Supporting Information S1, which includes data from Kurita et al., 2009). Monthly average precipitation $\delta^{18}O_p$ values are also significantly correlated with OLR ($r = 0.70$), GPCP precipitation ($r = -0.71$) and reanalysis E-P ($r = 0.62$) at the grid cells representing the sampling location (Figure S4 in Supporting Information S1). Precipitation $\delta^{18}O$ is also significantly, negatively correlated with precipitation amount at the CRRF collection site and the Koror weather station ($r = -0.70, -0.62$, respectively, Figure S4 in Supporting Information S1). E-P (ERA5 reanalysis) data from 2013 to 2023 averaged over the Palau site (nearest 7.5°N, 134.5°E) shows significant correlation with $\delta^{18}O_{sw}$ ($r = 0.44$) and salinity ($r = 0.41$) (Figure S4 in Supporting Information S1).

4. Discussion

4.1. Palau $\delta^{18}O_p$ as a Proxy for Tropical Pacific Hydroclimate

The $\delta^{18}O_p$ values of western tropical Pacific precipitation record aspects of regional convective activity, including precipitation amount (the 'amount effect'), the 'memory' and mixing of tropical air masses, changes in moisture transport, rain re-evaporation and moisture recycling, and stratiform rain versus convective rain amount (Aggarwal et al., 2016; Konecky et al., 2019; Kurita et al., 2009; Moerman et al., 2013; Risi et al., 2008). Most studies agree that, at least to some degree, $\delta^{18}O_p$ records from the western Pacific are indicative of large scale/regional hydroclimate processes rather than localized precipitation rates. However, the extensive list of driving mechanisms suggests that the degree to which any single process influences $\delta^{18}O_p$ is hard to define, and that temporal scale may be a further complicating factor.

Monthly Palau $\delta^{18}O_p$ values strongly track interannual variability in tropical Pacific hydroclimate (Figure S9 in Supporting Information S1). Palau $\delta^{18}O_p$ is negatively correlated with both station-based Koror weather station and GPCP precipitation amounts (Figure S4 in Supporting Information S1). In line with the concept of a 'regional amount effect,' where WPWP $\delta^{18}O_p$ is best correlated with regional, rather than local, precipitation amount (Konecky et al., 2019), the Palau $\delta^{18}O_p$—precipitation correlation is greatest with GPCP ($r = -0.71$) from the nearest $1° \times 1°$ grid point compared to station data.

Additionally, $\delta^{18}O_p$ is highly correlated with OLR, which is a proxy for tropical Pacific hydroclimate (Figure 3). Outgoing longwave radiation is a proxy for deep convective activity and precipitation that is tied to large-scale changes in SST in the tropical Pacific (Chiodi & Harrison, 2008; Graham & Barnett, 1987). As cloud cover and precipitation increase, OLR decreases. Positive correlations between OLR and $\delta^{18}O_p$ have been noted in several studies of tropical Pacific precipitation (Martin et al., 2018; Moerman et al., 2013; Permana et al., 2016). In Palau, we see this same positive correlation between monthly OLR and $\delta^{18}O_p$. Palau $\delta^{18}O_p$ and OLR are positively correlated over the WPWP ($r > \sim 0.6$), such that an increase in cloudiness (low OLR) coincides with lower Palau $\delta^{18}O_p$. Notably, $\delta^{18}O_p$ is negatively correlated with OLR in the central tropical Pacific as well ($r < \sim -0.6$). This pattern amounts to a Palau $\delta^{18}O_p$ signal that is broadly reflective of areas of convergence, convection and subsidence related to the Pacific Walker Circulation (PWC), which reinforces the spatial gradients in precipitation (OLR) via wind and pressure gradients across the tropical Pacific. This leads to a $\delta^{18}O_p$ signal that directly encodes high regional precipitation over the western Pacific and then indirectly records low central and eastern Pacific precipitation due to the coupled nature of the PWC.

4.2. The $\delta^{18}O_{sw}$ - $\delta^{18}O_p$ Relationship

$\delta^{18}O_{sw}$ values are often utilized and interpreted as proxies for ocean salinity and thus, atmospheric moisture balance (E—P). However, $\delta^{18}O_{sw}$ values retain much of their information about atmospheric processes through their relationship with precipitation isotope values ($\delta^{18}O_p$), which hold information beyond just E-P. To date, there is no observational evidence of a temporal relationship between $\delta^{18}O_p$ and $\delta^{18}O_{sw}$, although this is a common assumption. We find that monthly Palau $\delta^{18}O_{sw}$ values have a strong, positive correlation with Palau $\delta^{18}O_p$ ($r = 0.55$), suggesting that precipitation with lower $\delta^{18}O_p$ values leads to a lowering of $\delta^{18}O_{sw}$ locally (Figure 2). The strong relationship between $\delta^{18}O_{sw}$ and $\delta^{18}O_p$ suggests that the precipitation isotope signature at our site is distinct enough to impact the surface ocean chemistry. Furthermore, we see that $\delta^{18}O_{sw}$ is significantly negatively correlated with CRRF site-based, Koror weather station and GPCP nearest grid point precipitation amount ($r = -0.36, -0.39, -0.43$, respectively) (Figure S4 in Supporting Information S1). A negative correlation here shows that increased precipitation, which has a lower $\delta^{18}O$ value than seawater, subsequently lowers $\delta^{18}O_{sw}$ in Malakal Harbor. However, the precipitation amount—$\delta^{18}O_{sw}$ relationship is weaker than the $\delta^{18}O_p$—$\delta^{18}O_{sw}$

relationship, suggesting that the precipitation isotope signal is more impactful to $\delta^{18}O_{sw}$ than the precipitation amount itself. The $\delta^{18}O_p$ - $\delta^{18}O_{sw}$ relationship at Palau suggests that seawater may develop an isotopic signature of precipitation in regions of strong atmospheric convergence or where precipitation amounts are sufficiently high, such as the Indian Ocean or South Pacific Convergence Zone.

$\delta^{18}O_{sw}$ - $\delta^{18}O_p$ is more strongly correlated ($r = 0.55$) than salinity—$\delta^{18}O_p$ ($r = 0.35$), though both are significant (Figure S4 in Supporting Information S1). A stronger correlation between $\delta^{18}O_p$ and $\delta^{18}O_{sw}$ than $\delta^{18}O_p$ and salinity suggests that precipitation inputs into the surface ocean at our site are more distinct isotopically than volumetrically, the latter of which would directly affect salinity. This interpretation shifts away from a simplified 'high salinity, high evaporation, high $\delta^{18}O_{sw}$' versus 'low salinity, high precipitation, low $\delta^{18}O_{sw}$' framework. Precipitation in the WPWP is high compared to the global average, yet, precipitation inputs to the surface ocean are still small compared to global ocean volume. However, we see that the impact in isotopic space can be substantial, due to the large difference between mean seawater (~0‰) and precipitation values (here: ~−18 to 0‰).

Palau salinity does not appear to track tropical Pacific E-P or OLR as sensitively as Palau $\delta^{18}O_{sw}$ (example: Figure 3a vs. 3b). Generally, correlations between climatological variables and salinity are slightly lower or non-significant compared to the same correlations with $\delta^{18}O_{sw}$ (Figure S4 in Supporting Information S1). Correlations between monthly salinity and OLR are also weaker locally and regionally, with more areas of non-significant correlations present across the tropics (Figure 3). This disparity may point to a unique isotopic signature of deep convective activity associated with changes in OLR that is embedded in $\delta^{18}O_{sw}$ but is not discernible through salinity alone. The additional climate information from $\delta^{18}O_{sw}$ further suggests that seawater isotope data acts as a distinct tracer of regional hydroclimate in the ocean that provides more information than simply reconstructing salinity. $\delta^{18}O_{sw}$, through its relationship to $\delta^{18}O_p$, offers paleoclimatic insights into hydroclimatic processes in the WPWP.

4.3. El Niño Southern Oscillation Signals in Palau $\delta^{18}O_{sw}$

To summarize our findings thus far, there is a significant positive relationship between Palau $\delta^{18}O_{sw}$ and the NINO 3.4 index. Palau $\delta^{18}O_{sw}$ is also significantly correlated with $\delta^{18}O_p$ ($r = 0.55$), OLR around Palau ($r = 0.52$), and regional precipitation amount (GPCP, $r = -0.43$), each of which are influenced by changes in atmospheric convergence and convective precipitation during ENSO events. Therefore, these variables constitute the atmospheric influences of ENSO variability in the $\delta^{18}O_{sw}$ record. However, $\delta^{18}O_{sw}$ is also highly correlated with zonal and meridional flow in the mixed layer in the regions of the MC and NECC (Figure S7 in Supporting Information S1). Mindanao Current and NECC strength also changes in response to ENSO variability (Chen et al., 2021; Ren et al., 2020; Zhao et al., 2013, Figures S7, S8 in Supporting Information S1). The mechanism for this relationship is then an increased delivery of subtropical seawater (high $\delta^{18}O_{sw}$) during El Niño events and constitutes an oceanic contribution to the ENSO variability in the $\delta^{18}O_{sw}$ record. During a La Niña event, the reverse occurs. Combined with an atmospheric signal of decreased precipitation leading to reduced input of the comparatively lower $\delta^{18}O_p$ (Figures S11 in Supporting Information S1), the atmospheric and oceanic forcings on Palau $\delta^{18}O_{sw}$ form a constructive signal of higher $\delta^{18}O_{sw}$ during El Niño events. The constructive nature of this relationship is useful for developing ENSO proxies from marine carbonate records from this region, as it should amplify, not dampen, the ENSO signal. Further work to develop this relationship should include an assessment of the relative contribution of $\delta^{18}O_{sw}$ and SST to regional paleoclimate proxies and how that contribution changes during different ENSO events.

Finally, changes in the Palau $\delta^{18}O_{sw}$—salinity slope are also influenced by ENSO variability. Palau $\delta^{18}O_{sw}$ and salinity values have two visually identifiable secondary regressions that deviate from the bulk data relationship. The tenth quantile regression broadly corresponds to La Niña months ($y = 0.22$ ‰/PSU—7.50‰) as defined by NINO3.4, whereas the 90th quantile regression captures strong El Niño months ($y = 0.19$ ‰/PSU—6.22 ‰, Figure 4). The $\delta^{18}O_{sw}$—salinity slope is lower and has a higher intercept during El Niño months and the slope is higher with lower intercept during La Niña months. The lower slope in El Niño months can be attributed to a reduced range in $\delta^{18}O_{sw}$ from less $\delta^{18}O_p$ input to the surface ocean and/or fewer heavy rain events that carry extremely low $\delta^{18}O_p$. Contrastingly, the tenth quantile La Niña months likely have a lower intercept due to greater surface inputs of comparatively low $\delta^{18}O$ precipitation.

The $\delta^{18}O$ values of marine carbonates, such as corals, foraminifera, and giant clams, record the dual influence of $\delta^{18}O_{sw}$ and the temperature of the water in which they formed, and the balance of these contributions varies across

tropical Pacific (Thompson et al., 2022). Taking Indo-Pacific Warm Pool corals as an example, the contribution of $\delta^{18}O_{sw}$ to coral isotope records ($\delta^{18}O_c$) is significant enough that variability can be interpreted as salinity (Thompson et al., 2022). At Palau, driving mechanisms in the ocean and the atmosphere leading to constructive changes in $\delta^{18}O_{sw}$ in response to ENSO variability. However, the Palau $\delta^{18}O_{sw}$—salinity slope changes during ENSO phases. This finding complicates quantitative interpretations of paleo-$\delta^{18}O$ as salinity. We emphasize the need to consider calibrating $\delta^{18}O_{sw}$ to salinity with local $\delta^{18}O_{sw}$—salinity slopes, not only spatially, but also temporally (perhaps from isotope enabled climate models), at least for the interannual timescales investigated here. However, any approach to temporal or spatial constraint will require both significantly more observational data and the ability ground truth the modeled $\delta^{18}O_{sw}$—salinity through time.

5. Conclusions

Modern $\delta^{18}O_{sw}$ data serve the dual purpose of tracing hydroclimate processes and ocean circulation, providing a framework in which $\delta^{18}O$-based paleoclimate records can be interpreted. At Koror, Palau, concurrent time series of $\delta^{18}O_{sw}$ and $\delta^{18}O_p$ indicate $\delta^{18}O_{sw}$ values are strongly influenced by atmospheric processes, especially by $\delta^{18}O_p$ values. Changes in regional ocean circulation play a secondary role in driving $\delta^{18}O_{sw}$ variability, but this influence drives $\delta^{18}O_{sw}$ in the same direction as hydroclimate forcing on sub-decadal ENSO timescales. Although difficult to separate ocean circulation and atmospheric controls with this particular dataset, both Palau $\delta^{18}O_p$ and $\delta^{18}O_{sw}$ are highly correlated with ENSO indices reflecting basin-scale tropical Pacific climate variability, and therefore can serve as robust ENSO proxies. Notably, relationships between ENSO and atmospheric hydroclimate variables and Palau salinity tend to be weaker than those with isotope data. Quantile regressions of $\delta^{18}O_{sw}$—salinity reveal distinct signatures during La Niña and El Niño months, pointing to differences in primary processes driving $\delta^{18}O_{sw}$ during ENSO extremes. This work develops a framework for refining $\delta^{18}O$-based paleoclimate interpretations in the WPWP, demonstrating the utility of $\delta^{18}O_{sw}$ as a key hydroclimate variable that provides information about physical drivers not captured by salinity measurements.

Data Availability Statement

Precipitation and seawater isotope ($\delta^{18}O$, $\delta^{2}H$) data and salinity data are available at https://doi.org/10.60520/IEDA/113521 (Murray, 2025).

Acknowledgments
This research was funded by NSF 1203785 to JLC, KMC, and DC, and NSF 1847791 to JLC. We would like to thank our collaborators at the Coral Reef Research Station, Koror, Palau for their dedicated sample collection over the last decade.

References

Aggarwal, P. K., Romatschke, U., Araguas-Araguas, L., Belachew, D., Longstaffe, F. J., Berg, P., et al. (2016). Proportions of convective and stratiform precipitation revealed in water isotope ratios. *Nature Geoscience*, *9*(8), 624–629. https://doi.org/10.1038/ngeo2739

Akhoudas, C. H., Sallée, J.-B., Haumann, F. A., Meredith, M. P., Garabato, A. N., Reverdin, G., et al. (2021). Ventilation of the abyss in the atlantic sector of the southern ocean. *Scientific Reports*, *11*(1), 6760. https://doi.org/10.1038/s41598-021-86043-2

Bauch, D., Erlenkeuser, H., & Andersen, N. (2005). Water mass processes on Arctic shelves as revealed from $\delta^{18}O$ of H_2O. *Global and Planetary Change*, *48*(1–3), 165–174. https://doi.org/10.1016/j.gloplacha.2004.12.011

Bauch, D., Schlosser, P., & Fairbanks, R. (1995). Freshwater balance and the sources of deep and bottom waters in the Arctic Ocean inferred from the distribution of H2180. *Progress in Oceanography*, *35*, 28.

Chen, X., Qiu, B., Chen, S., & Qi, Y. (2021). Period-Lengthening of the Mindanao current variability from the long-term tide gauge sea level measurements. *JGR Oceans*, *126*(8), e2020JC016932. https://doi.org/10.1029/2020JC016932

Chiodi, A. M., & Harrison, D. E., (2008). Characterizing the interannual variability of the equatorial Pacific: An OLR perspective.

Conroy, J. L., Cobb, K. M., & Noone, D. (2013). Comparison of precipitation isotope variability across the tropical Pacific in observations and SWING2 model simulations. *Journal of Geophysical Research: Atmospheres*, *118*(11), 5867–5892. https://doi.org/10.1002/jgrd.50412

Conroy, J. L., Cobb, K. M., Lynch-Stieglitz, J., & Polissar, P. J. (2014). Constraints on the salinity–oxygen isotope relationship in the central tropical Pacific Ocean. *Marine Chemistry*, *161*, 26–33. https://doi.org/10.1016/j.marchem.2014.02.001

Conroy, J. L., Murray, N. K., Patterson, G. S., Schore, A. I. G., Ikuru, I., Cole, J. E., et al. (2023). Equatorial undercurrent influence on surface seawater $\delta^{18}O$ values in the Galápagos. *Geophysical Research Letters*, *50*(4), e2022GL102074. https://doi.org/10.1029/2022GL102074

Conroy, J. L., Noone, D., Cobb, K. M., Moerman, J. W., & Konecky, B. L. (2016). Paired stable isotopologues in precipitation and vapor: A case study of the amount effect within western tropical pacific storms: Isotopes in western pacific storms. *Journal of Geophysical Research: Atmospheres*, *121*(7), 3290–3303. https://doi.org/10.1002/2015JD023844

Conroy, J. L., Thompson, D. M., Cobb, K. M., Noone, D., Rea, S., & Legrande, A. N. (2017). Spatiotemporal variability in the $\delta^{18}O$-salinity relationship of seawater across the tropical Pacific Ocean: Isotope-salinity relationships. *Paleoceanography*, *32*(5), 484–497. https://doi.org/10.1002/2016PA003073

Dendy, J., Mesubed, D., Colin, P. L., Giardina, C. P., Cordell, S., Holm, T., & Uowolo, A. (2022). Dynamics of anthropogenic wildfire on Babeldaob island (Palau) as revealed by fire history. *Fire*, *5*(2), 45. https://doi.org/10.3390/fire5020045

Dubinina, E. O., Kossova, S. A., Miroshnikov, A. Y., & Kokryatskaya, N. M. (2017). Isotope (δD, $\delta^{18}O$) systematics in waters of the Russian Arctic seas. *Geochemistry International*, *55*(11), 1022–1032. https://doi.org/10.1134/S0016702917110052

Falster, G., Konecky, B., Madhavan, M., Stevenson, S., & Coats, S. (2021). Imprint of the pacific walker circulation in global precipitation $\delta^{18}O$. *Journal of Climate*, *34*, 19.

Graham, N. E., & Barnett, T. P. (1987). Sea surface temperature, surface wind divergence, and convection over tropical oceans. *Science*, *238*(4827), 657–659. https://doi.org/10.1126/science.238.4827.657

Grottoli, A. G., Adkins, J. F., Panero, W. R., Reaman, D. M., & Moots, K. (2010). Growth rates, stable oxygen isotopes (δ^{18}O), and strontium (Sr/Ca) composition in two species of Pacific sclerosponges (*Acanthocheatetes wellsi* and *Astrosclera willeyana*) with δ^{18} O calibration and application to paleoceanography. *Journal of Geophysical Research*, *115*(C6), 2009JC005586. https://doi.org/10.1029/2009JC005586

Horikawa, K., Kodaira, T., Zhang, J., & Obata, H. (2023). Salinity–oxygen isotope relationship during an El Niño (2014–2015) in the southwestern Pacific and comparisons with GEOSECS data (La Niña, 1973–1974). *Marine Chemistry*, *249*, 104222. https://doi.org/10.1016/j.marchem.2023.104222

Jean-Michel, L., Eric, G., Romain, B.-B., Gilles, G., Angélique, M., Marie, D., et al. (2021). The Copernicus global 1/12° oceanic and sea ice GLORYS12 reanalysis. *Frontiers in Earth Science*, *9*, 698876. https://doi.org/10.3389/feart.2021.698876

Konecky, B. L., Noone, D. C., & Cobb, K. M. (2019). The influence of competing hydroclimate processes on stable isotope ratios in tropical rainfall. *Geophysical Research Letters*, *46*(3), 1622–1633. https://doi.org/10.1029/2018GL080188

Kukla, T., Siler, N., Fiorella, R. P., Laguë, M. M., Hvam, C., Rugenstein, J. K. C., & Swann, A. L. S., (2024). Large isotope signals in tropical precipitation require large-scale changes in rainout. https://doi.org/10.22541/essoar.171536383.39550516/v1

Kurita, N., Ichiyanagi, K., Matsumoto, J., Yamanaka, M. D., & Ohata, T. (2009). The relationship between the isotopic content of precipitation and the precipitation amount in tropical regions. *Journal of Geochemical Exploration*, *102*(3), 113–122. https://doi.org/10.1016/j.gexplo.2009.03.002

Liebmann, B., & Smith, C. A. (1996). Description of a complete (interpolated) outgoing longwave radiation dataset. *Bulletin of the American Meteorological Society*, *77*, 1275–1277.

Martin, N. J., Conroy, J. L., Noone, D., Cobb, K. M., Konecky, B. L., & Rea, S. (2018). Seasonal and ENSO influences on the stable isotopic composition of galápagos precipitation: Stable isotopes in galápagos rainfall. *Journal of Geophysical Research: Atmospheres*, *123*(1), 261–275. https://doi.org/10.1002/2017JD027380

Moerman, J. W., Cobb, K. M., Adkins, J. F., Sodemann, H., Clark, B., & Tuen, A. A. (2013). Diurnal to interannual rainfall δ^{18}O variations in northern Borneo driven by regional hydrology. *Earth and Planetary Science Letters*, *369–370*, 108–119. https://doi.org/10.1016/j.epsl.2013.03.014

Morimoto, M., Abe, O., Kayanne, H., Kurita, N., Matsumoto, E., & Yoshida, N. (2002). Salinity records for the 1997–98 El Niño from western pacific corals. *Geophysical Research Letters*, *29*(11), 1540. https://doi.org/10.1029/2001GL013521

Murray, N. K. (2025). Palau temporal seawater isotope, precipitation isotope, and salinity data, Version 1.0. *Interdisciplinary Earth Data Alliance (IEDA)*. [dataset]. https://doi.org/10.60520/IEDA/113521

Murray, N. K., Muñoz, A. R., & Conroy, J. L. (2023). Machine learning solutions to regional surface ocean δ^{18} O-salinity relationships for paleoclimatic reconstruction. *Paleoceanography and Paleoclimatology*, *38*(9), e2023PA004612. https://doi.org/10.1029/2023PA004612

Osborne, M. C., Dunbar, R. B., Mucciarone, D. A., Druffel, E., & Sanchez-Cabeza, J.-A. (2014). A 215-yr coral δ^{18}O time series from Palau records dynamics of the West Pacific Warm Pool following the end of the Little Ice Age. *Coral Reefs*, *33*(3), 719–731. https://doi.org/10.1007/s00338-014-1146-1

Osborne, M. C., Dunbar, R. B., Mucciarone, D. A., Sanchez-Cabeza, J.-A., & Druffel, E. (2013). Regional calibration of coral-based climate reconstructions from Palau, west pacific warm pool (WPWP). *Palaeogeography, Palaeoclimatology, Palaeoecology*, *386*, 308–320. https://doi.org/10.1016/j.palaeo.2013.06.001

Permana, D. S., Thompson, L. G., & Setyadi, G. (2016). Tropical West Pacific moisture dynamics and climate controls on rainfall isotopic ratios in southern Papua, Indonesia: Tropical Rainfall Isotopes from Papua. *Journal of Geophysical Research: Atmospheres*, *121*(5), 2222–2245. https://doi.org/10.1002/2015JD023893

Rayner, N. A., Parker, D. E., Horton, E. B., Folland, C. K., Alexander, L. V., Rowell, D. P., et al. (2003). Global analyses of sea surface temperature, sea ice, and night marine air temperature since the late nineteenth century. *Journal of Geophysical Research*, *108*, 4407. https://doi.org/10.1029/2002jd002670

Reed, E. V., Thompson, D. M., & Anchukaitis, K. J. (2022). Coral-based sea surface salinity reconstructions and the role of observational uncertainties in inferred variability and trends. *Paleoceanography and Paleoclimatology*, *37*(6). https://doi.org/10.1029/2021PA004371

Ren, Q., Li, Y., Wang, F., Duan, J., Hu, S., & Wang, F. (2020). Variability of the Mindanao current induced by El Niño events. *Journal of Physical Oceanography*, *50*(6), 1753–1772. https://doi.org/10.1175/JPO-D-19-0150.1

Reyes-Macaya, D., Hoogakker, B., Martínez-Méndez, G., Llanillo, P. J., Grasse, P., Mohtadi, M., et al. (2022). Isotopic characterization of water masses in the southeast pacific region: Paleoceanographic implications. *JGR Oceans*, *127*(1), e2021JC017525. https://doi.org/10.1029/2021JC017525

Risi, C., Bony, S., & Vimeux, F. (2008). Influence of convective processes on the isotopic composition (δ^{18}O and δD) of precipitation and water vapor in the tropics: 2. Physical interpretation of the amount effect. *Journal of Geophysical Research*, *113*(D19), D19306. https://doi.org/10.1029/2008JD009943

Schmitt, S. R., Riveros-Iregui, D. A., & Hu, J. (2018). The role of fog, orography, and seasonality on precipitation in a semiarid, tropical island. *Hydrological Processes*, *32*(18), 2792–2805. https://doi.org/10.1002/hyp.13228

Thompson, D. M., Conroy, J. L., Konecky, B. L., Stevenson, S., DeLong, K. L., McKay, N., et al. (2022). Identifying hydro-sensitive coral δ^{18}O records for improved high-resolution temperature and salinity reconstructions. *Geophysical Research Letters*, *49*(9). https://doi.org/10.1029/2021GL096153

van Geldern, R., & Barth, J. A. C. (2012). Optimization of instrument setup and post-run corrections for oxygen and hydrogen stable isotope measurements of water by isotope ratio infrared spectroscopy (IRIS): Water stable isotope analysis with IRIS. *Limnology and Oceanography: Methods*, *10*(12), 1024–1036. https://doi.org/10.4319/lom.2012.10.1024

Wen, H., Yan, H., Liu, C., Zhao, N., Liu, S., Dodson, J., et al. (2024). Seasonal to interannual variations of daily growth rate of a Tridacna shell from Palau Island, western Pacific, and paleoclimatic implications. *Palaeogeography, Palaeoclimatology, Palaeoecology*, *647*, 112258. https://doi.org/10.1016/j.palaeo.2024.112258

Wu, H. C., & Grottoli, A. G. (2010). Stable oxygen isotope records of corals and a sclerosponge in the Western Pacific warm pool. *Coral Reefs*, *29*(2), 413–418. https://doi.org/10.1007/s00338-009-0576-7

Zhao, J., Li, Y., & Wang, F. (2013). Dynamical responses of the west pacific north equatorial countercurrent (NECC) system to El Niño events: Responses of NECC system to El NiÑos. *Journal of Geophysical Research: Oceans*, *118*(6), 2828–2844. https://doi.org/10.1002/jgrc.20196